Chemical abundance analysis of symbiotic giants. RW Hya, SY Mus, BX Mon, and AE Ara

Cezary Galan[1], Joanna Mikolajewska[1], Kenneth H. Hinkle[2], Miroslaw R. Schmidt[3], and Mariusz Gromadzki[4]

[1]N. Copernicus Astronomical Center, Bartycka 18, PL-00-716 Warsaw, Poland, (E-mail: cgalan@camk.edu.pl)
[2]National Optical Astronomy Observatory, P.O. Box 26732, Tucson, AZ 85726, USA
[3]N. Copernicus Astronomical Center, Rabiańska 8, PL-87-100 Toruń, Poland
[4]Departamento de Física y Astronomía, Universidad de Valparaíso, Av. Gran Bretaña 1111, Playa Ancha, Casilla 5030, Chile

Introduction

Symbiotic stars are long period binary systems, composed of two evolved and strongly interacting stars: a red giant and a hot and luminous, typically white dwarf, companion surrounded by an ionized nebula. Mass loss from the giant undergoes accretion to the compact object via wind and/or Roche lobe overflow (e.g., [20], [19]) resulting in the formation of accretion discs and jets (e.g., [22], [30], [1]). The hot companion was previously a red giant and this mass transfer episode, in the opposite direction, should have left traces in the chemical composition of the current red giant. Symbiotic stars can be progenitors for Supernovae Type Ia and can be responsible for several or perhaps up to about thirty percent of these events (e.g., [7], [19]).

The complex structure including the many kinds of interactions make symbiotic stars excellent laboratories for studying various aspects of the late stages of binary evolution including those that impact the chemical evolution of the Galaxy and the formation of stellar populations. Knowledge of the chemical composition of symbiotic giants is essential to advancing our understanding but unfortunately reliable determinations exist in a few cases. Thus far, analysis of the photospheric chemical abundances have been performed for four only normal S-type symbiotic giants (V2116 Oph [12], T CrB, RS Oph [33] and CH Cyg [23]). In all these cases solar or nearly solar metallicities were found. Some information about chemical composition is also available for roughly a dozen so called yellow symbiotic systems. These are S-type symbiotics containing a giant of K or G spectral type that is metal poor with overabundant s-process elements (AG Dra [24], BD-21 3873, [25], Hen 2-467 [27], CD-43 14304, Hen 3-1213, Hen 3-863, StHA 176 [29]). Compositions also have been measured for members of the small D' subclass of symbiotic stars that contain fast rotating G-type giants and warm dust shells. These have solar metallicities with overabundant s-process elements (StHA 190 [26], HD 330036, AS 201 [28]). The number of objects is too small for statistical considerations.

We have started a chemical composition analysis for a sample of over 30 symbiotic systems. Here we present the results obtained thus far for four objects: RW Hya, SY Mus, BX Mon and AE Ara.

Observations and data reduction

The observational data are high-resolution ($R = \lambda/\Delta\lambda \sim 50000$; S/N ≥ 100), near-IR spectra collected with the Phoenix cryogenic echelle spectrometer on the 8 m Gemini South telescope during the years 2003–2006. The spectra cover narrow wavelength ranges (∼100Å) located in the H and K photometric bands at mean wavelengths 1.563 μm, 2.225 μm, and 2.361 μm (hereafter H, K, and K'-band spectra, respectively). The H-band spectra contain molecular CO and OH lines, K-band spectra CN lines, with both ranges useful for abundances of carbon, nitrogen and oxygen and elements around iron peak: Sc, Ti, Fe, Ni. The K'-band spectra are dominated by strong CO features that enable measurement of the $^{12}C/^{13}C$ isotopic ratio. The spectra were extracted and wavelength calibrated using standard reduction techniques [13] and all were heliocentric corrected. In all cases telluric lines were either not present in the interval observed or were removed by reference to a hot standard star. The Gaussian instrumental profile is in all cases about 6 km s^{-1} FWHM corresponding to instrumental profiles of 0.31Å , 0.44Å and 0.47Å in the case of the H-band, K-band, and K'-band spectra, respectively. The log of our spectroscopic observations is given in the table below.

Object	Sp. Region Band (λ[μm])	Date	HJD	Orb. Phase
RW Hya	H (~1.56)	16.02.2003	2452686.8380	0.57
	K (~2.23)	20.04.2003	2452749.6295	0.74
	K (~2.23)	13.12.2003	2452986.8656	0.38
	K' (~2.36)	3.04.2006	2453828.6308	0.65
SY Mus	H (~1.56)	17.02.2003	2452687.7566	0.02
	K (~2.23)	20.04.2003	2452749.5817	0.12
	K (~2.23)	13.12.2003	2452986.8250	0.50
	K' (~2.36)	3.04.2006	2453828.5767	0.84
BX Mon	H (~1.56)	16.02.2003	2452686.7409	0.30
	K (~2.23)	20.04.2003	2452749.5231	0.35
	K' (~2.36)	3.04.2006	2453828.5095	0.20
AE Ara	H (~1.56)	17.02.2003	2452687.8830	0.05
	K (~2.23)	20.04.2003	2452749.8669	0.13
	K (~2.23)	3.04.2004	2453098.8487	0.56

References

[1] Angeloni, R., et al., 2011, *ApJ*, 743, 8
[2] Asplund, M., Grevesse, N., Sauval A., & Scott, P., 2009, *ARAA* 47, 481
[3] Bensby, T., & Feltzing, S., 2006, *MNRAS*, 397, 1
[4] Brandt, S., 1998, *Data Analysis, Statistical and Comput. Methods*, (PWN)
[5] Carlberg, J.K., Majewski, S.R., Patterson, R.J., et al., 2011, *ApJ*, 732, 39
[6] Cunha, K., & Smith, V.V., 2006, *ApJ*, 651, 491
[7] Dilday, B., et al., 2012, *Science*, 337, 942
[8] Fekel, F.C., Hinkle, H.K., Joyce, R.R., et al., 2003, *ASPC*, 303, 113
[9] Feltzing, S., Bensby, T., & Lundstrom, I., 2003, *A&A*, 397, 1
[10] Goorvitch, D., 1994, *ApJS*, 95, 535
[11] Gustafsson, B., Edvardsson, B., Eriksson, K., et al., 2008, *A&A*, 486, 951
[12] Hinkle, K.H., Fekel, F.C., Joyce, R.R., et al., 2006, *ApJ*, 641, 479
[13] Joyce, R., 1992, *ASPC*, 23, 258
[14] Kucinskas, A., Hauschildt, P.H., Ludwig, H.-G., et al., 2005, *A&A*, 442, 281
[15] Kupka, F., Piskunov, N., Ryabchikova, T., et al., 1999, *A&AS*, 138, 119
[16] Kurucz, R.L., *http://kurucz.harvard.edu/*
[17] Melendez, J., & Barbuy, B., 1999, *ApJS*, 124, 527
[18] Mürset, U., & Schmidt, H.M., 1999, *A&ASS*, 137, 473
[19] Mikolajewska, J., 2012, *Baltic Astronomy*, 21, 5
[20] Podsiadlowski Ph., & Mohamed S., 2007, *Baltic Astronomy*, 16, 26
[21] Richichi, A., Fabbroni, L., Ragland, S., Scholz, M., 1999, *A&A*, 344, 511
[22] Solf, J., & Ulrich, H., 1985, *A&A*, 148, 274
[23] Schmidt, M.R., Zacs, L., Mikolajewska, J., & Hinkle, K., 2006, *A&A*, 446, 603
[24] Smith, V.V., Cunha, K., Jorissen, A., & Boffin, H.M.J., 1996, *A&A*, 315, 179
[25] Smith, V.V., Cunha, K., Jorissen, A., & Boffin, H.M.J., 1997, *A&A*, 324, 97
[26] Smith, V.V., Pereira, C.B., Cunha, K., 2001, *ApJ*, 556, 55
[27] Pereira, C.B., Smith, V.V.; Cunha, K., 1998, *AJ*, 116, 1977
[28] Pereira, C.B., Smith, V.V.; Cunha, K., 2005, *A&A*, 429, 993
[29] Pereira, C.B., & Roig, F., 2009, *AJ*, 137, 118
[30] Tomov T., 1985, *ASPC*, 303, 376
[31] van Belle, G.T., Lane, B.F., Thompson, R.R., et al., 1999, *AJ*, 117, 521
[32] van Leeuwen, F., 2007, *A&A*, 474, 653
[33] Wallerstein, G., Harrison, T., Munari, U., Vanture, A., 2008, *PASP*, 120, 492

Methods

The standard LTE analysis

The abundance analyses were performed by fitting synthetic spectra to observed ones with a method similar to that used for CH Cyg by Schmidt et al. [23]. Standard *LTE* analysis and *MARCS* model atmospheres developed by Gustafsson et al. [11] were used for the spectral synthesis. The code *WIDMO* developed by M.R. Schmidt was used to calculate synthetic spectra over the observed spectral regions. To perform a χ^2 minimization, a special overlay was developed on the *WIDMO* code with use of the simplex algorithm [4]. Use of this procedure, in our case, enables an improvement of about ten times in the computation efficiency. The atomic data were taken from the *VALD* database [15] in the case of K- and K'-band regions and from the list given by Melendez & Barbuy [17] for the H-band region. For the molecular lines we used the line lists published by Goorvitch [10] (CO) and from CD-ROMs of Kurucz [16] (CN and OH).

Input stellar parameters

The input effective temperatures $T_{\rm eff}$ were estimated from the known spectral types [18] adopting the calibration by Richichi et al. [21] and van Belle et al. [31] (see table below). From the infrared colors and color excesses we obtained intrinsic colors. Using the Kucinskas et al. [14] $T_{\rm eff}$–log g–*color* relation for late-type giants, we estimated surface gravities and effective temperatures that are in good agreement with those from the spectral types. We then used model atmospheres for the estimated values of surface gravities and the effective temperature set to $T_{\rm eff}$=3700 K for RW Hya and $T_{\rm eff}$=3400 K for SY Mus, BX Mon and AE Ara. The macroturbulence velocity $\zeta_{\rm t}$ was set at 3 km/s, a value typical for the cool red giants (e.g. [8]).

Object	Spectral Type [18]	$T_{\rm eff}$ [K] [21]	$T_{\rm eff}$ [K] [31]	J-K	$E(B$-$V)$	$(J$-$K)_0$	$T_{\rm eff}$ [K] [14]	log g [14]
RW Hya	M2	3655 ± 80	3750 ± 22	1.15	0.02-0.10	~1.1	3600 – 3700	0.5
SY Mus	M5	3355 ± 75	3424 ± 30	1.40	0.40-0.50	~1.2	≲3500	0.5
BX Mon	M5.5	3300 ± 75	3400 ± 30	1.37	0.10-0.20	~1.3	~3300	0.0
AE Ara	M5.5	3300 ± 75	3400 ± 30	1.36	0.20-0.30	~1.25	~3300	0.0

The radial velocities for individual spectra were obtained with a cross-correlation technique similar to that of Carlberg et al. [5] but with synthetic spectra as the template. Rotational velocities were estimated via direct measurement of the FWHM of the 6 relatively strong, unblended atomic lines (Ti I, Fe I, Sc I) present in the K-band region, the same lines used by Fekel et al. [8]. The resulting values of the radial and rotational velocities were set as a fixed parameters in our solutions.

Procedure to derive abundances

The following procedure was adopted to carry out the abundance solution.

- Estimation of the initial values of the abundance parameters:
  - initially the solar composition [2] was adopted
  - fitting by eye, alternately the OH, CO, CN and atomic lines
- Building of the $n+1$, n dimensional sets of free parameters – the so called simplex
- Minimization with the simplex algorithm:
  - 9 different simplexes were used, with different microturbulent velocity $\xi_{\rm t}$ values (sampled in the range 1.2–2.6 km/s) to obtain optimal fit to H- and K-band spectra
  - searching for $^{12}C/^{13}C$ by fitting to K'-band spectrum
  - reconciliation of ^{12}C and $^{12}C/^{13}C$ within $\leq$3 iterations

Results

The final derived abundances for CNO elements and atomic lines (Sc I, Ti I, Fe I, Ni I) on the scale $\log\epsilon(X) = logN(X)N(H)^{-1} + 12.0$, the isotopic ratios $^{12}C/^{13}C$, microturbulences $\xi_{\rm t}$ and projected rotational velocities $V_{\rm rot}\sin i$, are summarized in the table below together with formal uncertainties. Our analysis of the chemical abundances reveals a significantly subsolar metallicity (Me/H ∼ −0.75) for RW Hya, slightly subsolar metallicities in BX Mon and AE Ara, and an approximately solar metallicity in SY Mus. The $^{12}C/^{13}C$ isotopic ratios are low: ∼6, ∼10, and ∼9, for RW Hya, SY Mus, and BX Mon respectively.

	RW Hya		SY Mus		BX Mon		AE Ara	
X	log $\epsilon(X)$	$[X]$	log $\epsilon(X)$	$[X]$	log $\epsilon(X)$	$[X]$	log $\epsilon(X)$	$[X]$
^{12}C	7.53±0.02	-0.90±0.07	8.17±0.01	-0.26±0.06	7.79±0.01	-0.64±0.06	8.06±0.01	-0.37±0.06
N	7.46±0.03	-0.37±0.08	8.11±0.02	+0.28±0.07	7.89±0.02	+0.06±0.07	8.05±0.02	+0.22±0.07
O	8.17±0.01	-0.52±0.06	8.66±0.01	-0.03±0.06	8.37±0.01	-0.32±0.06	8.62±0.02	-0.07±0.07
Sc	2.71±0.05	-0.44±0.09	3.97±0.05	+0.82±0.09	3.82±0.11	+0.67±0.15	4.62±0.14	+1.47±0.18
Ti	4.49±0.05	-0.46±0.10	5.12±0.03	+0.17±0.08	4.96±0.06	+0.01±0.11	5.43±0.07	+0.48±0.12
Fe	6.74±0.02	-0.76±0.06	7.42±0.02	-0.08±0.06	7.16±0.02	-0.34±0.06	7.32±0.02	-0.18±0.06
Ni	5.63±0.03	-0.59±0.07	6.37±0.03	+0.15±0.07	6.18±0.05	-0.04±0.09	6.15±0.09	-0.07±0.13
$^{12}C/^{13}C$	~6.2	...	~10.4	...	~8.6	...	...	...
$\xi_{\rm t}$	1.8±0.2		2.0±0.2		1.8±0.2		1.8±0.2	
$V_{\rm rot}\sin i$	6.3±0.4		6.6±0.3		8.5±0.5		11.0±0.3	

The final synthetic fits to the spectra of RW Hya and BX Mon:

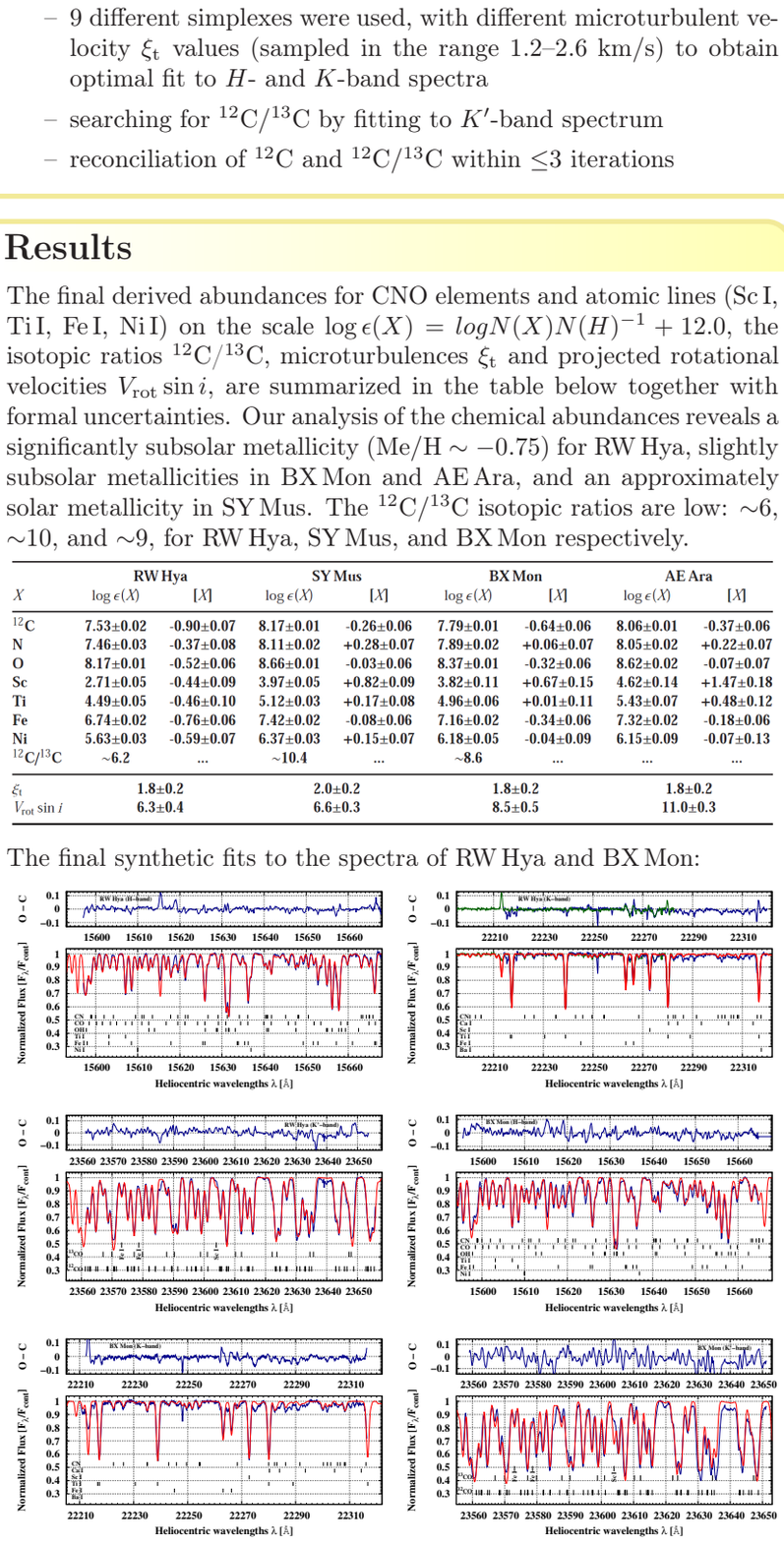

Symbiotic stars in Galactic populations

The chemical composition analysis of the four symbiotic giants enables a comparison of their chemical properties to those of Galactic stellar populations previously obtained by various authors. In the table below are abundances and estimates of their ratios obtained by us for RW Hya, SY Mus, BX Mon and AE Ara and those obtained by Schmidt et al. [23] for CH Cyg.

	A(^{12}C)	A(^{14}N)	[C/O]	[C/Fe]	[O/H]	[O/Fe]	[Fe/H]	[Ti/Fe]	References
RW Hya	7.53	7.46	-0.38	-0.14	-0.52	0.24	-0.76	0.30	this work
SY Mus	8.17	8.11	-0.23	-0.18	-0.03	0.05	-0.08	0.25	this work
BX Mon	7.79	7.89	-0.32	-0.30	-0.32	0.02	-0.34	0.35	this work
AE Ara	8.06	8.05	-0.30	-0.19	-0.07	0.11	-0.18	0.66	this work
CH Cyg	8.37	8.08	-0.08	-0.15	-0.07	-0.07	0.00	0.22	[23]

We show the positions of these stars in the diagrams below with large dots in blue, green, purple, orange, and red for RW Hya, SY Mus, BX Mon, AE Ara, and CH Cyg respectively (according to the convention in the table above).

Bensby & Feltzing (fig. 11–[3]) present an analysis of the trends of [C/Fe] and [C/O] versus [Fe/H] and [O/H] present in various Galactic populations as a result of chemical evolution. While the [C/Fe]–[Fe/H] relation is totally merged and flat the others show clear separation between thin- (open circles) and thick-disc (filled circles and triangles) populations. The uncertainties in the positions are quite large (∼ 0.2-0.3), nevertheless we can see the RW Hya system (proper motions suggest membership of the thick-disc or halo populations), placed far away from the positions of the other systems, that in most cases seem fall into regions dominated by thin-disc stars.

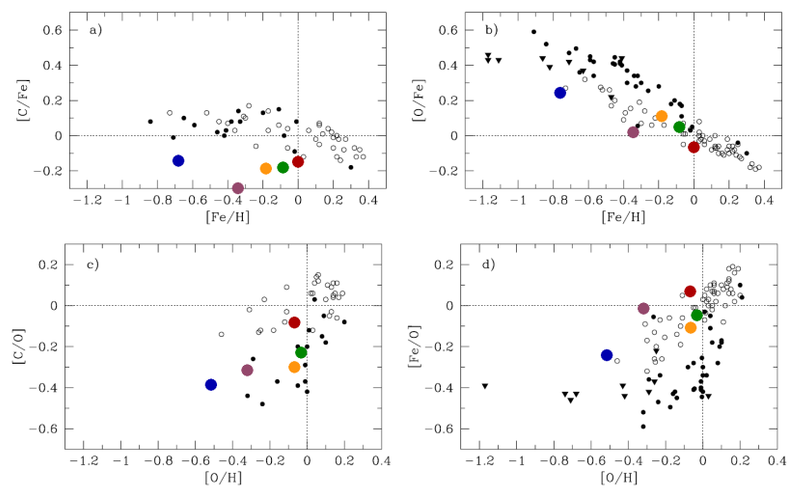

On the left below is shown the relation [Ti/Fe]–[Fe/H] from Cunha & Smith (2006, fig. 11–[6]) for stars of different populations: disc stars (open, blue circles), LMC (magenta squares), Sculptor (magenta circles), Galactic bulge (pentagons with errorbars). The position of AE Ara on this diagram appears to confirm membership in the bulge population. On the right the CN cycle is shown (fig. 4–[6]). All of our stars analyzed so far fall into the ^{14}N-rich zone. This is further evidence, in addition to the low $^{12}C/^{13}C$ isotopic ratios, that the first-dredge up has occurred in these objects.

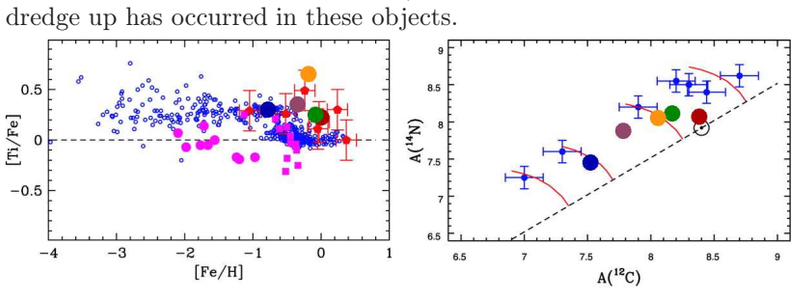

The Galactic coordinates, distances and proper motions for the four symbiotic systems enable us to estimate their Galactic velocities (U,V,W - table below) and to analyze their position on the Toomre diagram (figure below). We used fig. 1 from Feltzing et al. [9] with denoted positions of thin- (open circles), thick-disc (filled circles and open squares), and halo stars (asterisks). The RW Hya system is placed in the extended thick-disk contrary to the other three symbiotic systems that are placed in the thin-disc population.

	Galactic coordinates [degrees] l	b	Distance [pc] d	References for distance	Proper motion [mas/yr] $\mu_l \cos b$	μ_b	Systemic velocity [km/s] γ	Galactic velocities (U,V,W) [km/s] U	[km/s] V	[km/s] W
RW Hya	315.0	36.5	1700	this work	-15.3	17.6	12.4	-142.2	-34.5	121.6
SY Mus	294.8	3.8	1600	this work	4.8	-0.7	12.9	39.2	3.4	-4.2
BX Mon	220.0	5.9	2500	this work	2.9	-3.3	29.1	-3.8	-47.4	-36.2
CH Cyg	81.9	15.6	243	[32]	-21.1	-1.6	-57.7	16.2	-58.0	-17.3

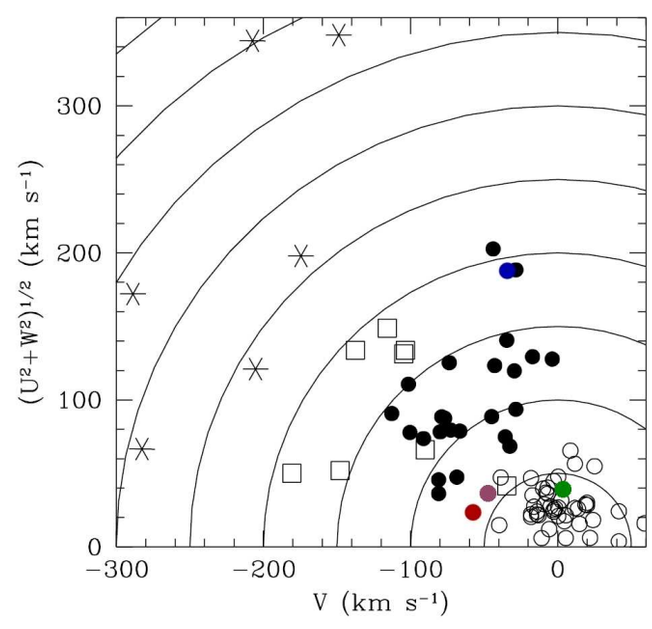

We expect that an analysis like that presented above when applied to a statistically significant sample will allow a better understanding of the chemical evolution of symbiotic systems in various stellar populations.

Acknowledgements

This study is partly supported by the Polish National Science Centre grants No DEC-2011/01/B/ST9/06145 and No DEC-2013/08/S/ST9/00581. MG is financed by the GEMINI-CONICYT Fund allocated to the project 32110014. CG gratefully acknowledges A. Smith for careful reading of the manuscript.